

Broadband dichromatic variational measurementSergey P. Vyatchanin ^{1,2,*}, Albert I. Nazmiev ¹ and Andrey B. Matsko ³¹*Faculty of Physics, M. V. Lomonosov Moscow State University, Leninskie Gory, Moscow 119991, Russia*²*Quantum Technology Centre, M. V. Lomonosov Moscow State University, Leninskie Gory, Moscow 119991, Russia*³*Jet Propulsion Laboratory, California Institute of Technology, 4800 Oak Grove Drive, Pasadena, California 91109-8099, USA*

(Received 10 May 2021; accepted 5 August 2021; published 24 August 2021)

The standard quantum limit (SQL) of a classical mechanical force detection results from quantum backaction impinging by the meter on a probe mechanical transducer perturbed by the force of interest. In this paper we introduce a technique of continuous broadband backaction, avoiding measurements for the case of a resonant signal force acting on a linear mechanical oscillator supporting one of the mirrors of an optical Michelson-Sagnac interferometer (MSI). The interferometer with the movable mirror is an optomechanical transducer able to support the polychromatic probe field. The method involves a dichromatic optical probe resonant with the MSI modes and having frequency separation equal to the mechanical frequency. We show that analyzing each of the harmonics of the probe reflected from the mechanical system separately and postprocessing the measurement results allows excluding the backaction in a broad frequency band and measuring the force with sensitivity better than the SQL.

DOI: [10.1103/PhysRevA.104.023519](https://doi.org/10.1103/PhysRevA.104.023519)**I. INTRODUCTION**

Optical transducers are frequently used for observation of mechanical motion. They allow measuring displacement, speed, acceleration, and rotation of mechanical systems. Mechanical motion can change the frequency, the amplitude, and the phase of the probe light, which are processed to obtain information about the motion. The measurement sensitivity can be extremely high. For instance, a relative mechanical displacement that is orders of magnitude smaller than a proton size can be detected. This feature is utilized in gravitational wave detectors [1–6], in magnetometers [7,8], and in torque sensors [9–11].

The fundamental sensitivity limitations of the measurement always were of interest. One of the limits results from the fundamental thermodynamic fluctuations of the probe mechanical system. The absolute position detection is restricted due to the Nyquist noise. However, this obstacle can be removed if one intends to measure a variation of the position, not its absolute value. The thermal noise does not limit the sensitivity of the measurement that occurs much faster than the system ringdown time.

Another limitation comes from the quantum noise of the meter. On one hand, the accuracy of the measurements of the observables of the meter is restricted because of their fundamental quantum fluctuations, represented by the shot noise for the optical probe wave. On the other hand, the sensitivity is impacted by the perturbation of the state of the probe mass due to the mechanical action of the meter on the mass. This effect is called “quantum backaction.” In the case of the optical meter, the mechanical perturbation results from the pressure of light. Interplay between these two

phenomena results in the so-called standard quantum limit (SQL) [12,13] of the measurement sensitivity.

The value of the SQL depends on the measurement system as well as the measurement strategy and the measurement observable. In the case of the detection of a classical force acting on a mechanical probe mass, the SQL can be avoided in a configuration supporting optomechanical velocity measurement [14,15]. The limit also can be surpassed using opto-mechanical rigidity [16–18]. Preparation of the probe light in a nonclassical state [19–25] as well as detection of a variation of a strongly perturbed optical quadrature [26–28] curbs the quantum backaction and lifts the SQL. The backaction and the SQL can be avoided with coherent quantum noise cancellation [29–31] as well as compensation using an auxiliary medium with negative nonlinearity [32].

Optimization of the detection scheme by utilizing a few optical frequency harmonics as a probe allows beating the SQL of a force detection. The technique was introduced 40 years ago [33,34] and then expanded to various measurement configurations involving only one optical resonant mode [35–39] as well as configurations involving two modes [29,40]. Additionally, usage of a dichromatic optical probe in a resonant optical transducer may lead to the observation of phenomena such as negative radiation pressure [41,42], optical quadrature-dependent quantum backaction [26,28,43,44], and mechanical velocity-dependent interaction [14,15]. All these phenomena are useful for backaction suppression.

Noncommutativity between the probe noise and the quantum backaction noise is the reason for the SQL. In a simple displacement sensor the probe noise is represented by the phase noise of light and the backaction noise depends on the amplitude noise of light. The signal is contained in the phase of the probe. The relative phase noise decreases with optical power. The relative backaction noise increases with the power. The signal-to-noise ratio optimizes at a specific power

*Corresponding author: svyatchanin@phys.msu.ru

value. The optimal measurement sensitivity corresponds to the SQL. Because phase and amplitude quantum fluctuations of the same wave do not commute, it is not possible to measure the amplitude noise and subtract it from the measurement result.

In this paper we suggest an alternative measurement procedure, in which the experimenter uses a dichromatic optical probe (i.e., *two* optical modes, separated by a mechanical resonator frequency, are pumped). It provides the important possibility to detect amplitude (or phase) quadratures of *two* outputs from each mode *independently*. These quadratures are entangled due to ponderomotive interaction with the mechanical oscillator. In particular, we propose to measure the sum and the difference, for example, of amplitude quadratures, because the sum contains backaction without any information on the mechanical degree of freedom, whereas the difference of amplitude quadratures contains information on the mechanical degree with backaction. This allows postprocessing of the measurement result and subtracting the quantum backaction contribution *completely*, not only in some bandwidth as in conventional variational measurement [26,28,43]. This is the main advantage of the proposed procedure.

In the measurement procedure the probe mass is strongly perturbed. In this way the technique is similar to the variational approach, leading to the accurate measurement of a variation of a quantum system despite the strong perturbation of the system parameters. Unlike the standard variational measurement, the technique described here is broadband. The backaction can be removed at all spectral frequencies.

The technique proposed here is especially efficient when the signal force is resonant with the mechanical probe mass suspension. In this regime the external force modifies the power redistribution between the probe spectral components most efficiently. The variational measurement technique based on a monochromatic probe light does not perform well in this case.

The paper is organized as follows. The physical model of the measurement system is introduced in Sec. II. The mean amplitudes of the system parameters, the quantum fluctuations, and the associated noise components are studied in Sec. III. The optimal sensitivity of the measurement is also found in Sec. III. The impact of the parasitic sidebands is analyzed in Sec. IV. Section V concludes the paper.

II. PHYSICAL MODEL

Let us consider an optomechanical system consisting of two externally pumped optical modes coupled with each other and with a mechanical oscillator. The difference between the optical mode frequencies is equal to the frequency of the mechanical oscillator. In this case the mechanical oscillation signal that appeared in one mode became resonance for another one—see (2.9) below. In what follows we show the feasibility of the broadband detection of a small signal force acting on the mechanical oscillator while keeping the sensitivity of the measurement better than that of the SQL.

The optomechanical system can be realized in a ring cavity with coupled clockwise and counterclockwise modes (Fig. 1). The uncoupled modes are frequency degenerate. Let us assume that their frequency is equal to ω_0 . Introducing a *low*

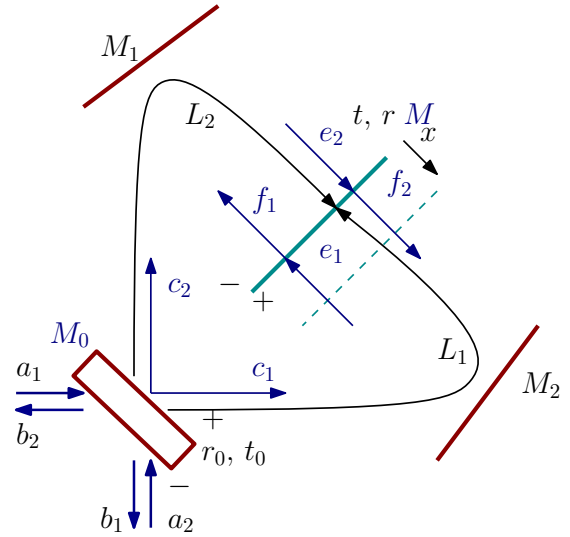


FIG. 1. High-finesse ring cavity with the input mirror M_0 with transmission t_0 and reflectivity r_0 ($t_0 \ll r_0$) and the dielectric mirror M (membrane) inside with transmission t and reflectivity r ($r \ll t$).

reflecting membrane (with transmittivity t and reflectivity r) inside the cavity removes degeneracy and eigenfrequencies ω_{\pm} of the modes split (so-called coherent coupling [45]):

$$\omega_{\pm} = \omega_0 \pm |\kappa|, \quad \kappa = \frac{rce^{i\phi}}{t(L_1 + L_2)}, \quad r \ll t, \quad (2.1)$$

where the splitting factor κ is a complex value. A specific feature of coherent coupling is that the absolute value of $|\kappa|$ depends on optical parameters of the membrane and its phase of ϕ depends on the membrane position [45]. For resonance the optomechanical interaction mechanical frequency ω_m should be equal to the splitting between optical modes: $2|\kappa| = \omega_m$.

Another example of a scheme enabling the backaction evading measurement is the Michelson-Sagnac interferometer (MSI) shown in Fig. 2. The system also has two degenerate modes. If the position of a perfectly reflecting mirror M is fixed, one MSI mode, characterized by the frequency ω_+ , is

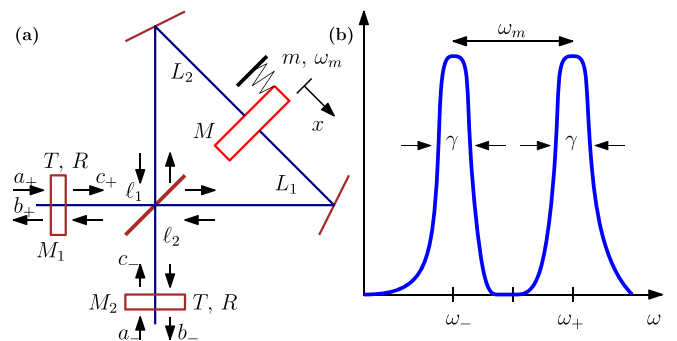


FIG. 2. (a) Schematic of the Michelson-Sagnac interferometer in which the mirror M is totally reflecting. The mirror is a test mass m of the mechanical oscillator with the frequency ω_m . (b) Two eigenmodes with the frequencies ω_- and ω_+ are coupled with the mechanical oscillator. The relaxation rate γ is the same for both modes, $\gamma \ll \omega_m$. Modes ω_{\pm} are resonantly pumped.

given by a light wave which travels between M_1 and the beam splitter (BS). The light is split on the BS and after reflection from the mirror M returns exactly to M_1 . It does not propagate to M_2 . The other mode, characterized by the frequency ω_- , is represented by a wave which travels from M_2 to the BS and after reflection from M returns to M_2 and does not propagate to M_1 . The frequencies of the modes, ω_{\pm} , are controlled by the variation of the path distances ℓ_1 and ℓ_2 . Variation of the position of the mirror M provides coupling between the modes. The mirror M is a test mass of the mechanical oscillator with the mass m and the eigenfrequency ω_m .

One can show that both optomechanical schemes in Figs. 1 and 2 are described by similar Hamiltonians—see the Hamiltonian for the scheme in Fig. 1 derived in Appendix A and Eqs. (2.4) below. The advantages of the scheme shown in Fig. 2 include the following.

(i) One is capable of tuning the scheme without mirrors M_1 and M_2 , selecting the position of the mirror M so that the MSI becomes nontransparent. Light from the left and right ports reflects without mixing up unless a force is applied to the mirror.

(ii) Adding mirrors M_1 and M_2 defines the eigenfrequency of the modes ω_{\pm} . By shifting the position, for example, of the mirror M_1 , one can tune the difference of frequencies to realize the resonance condition $\omega_+ - \omega_- = \omega_m$.

(iii) The outputs of each mode are separated in space, enabling the measurement of the light in each output independently.

The technique proposed here is similar to the earlier introduced two-frequency probe-based measurement strategy in which a nondegenerate optical parametric amplification was utilized to achieve the coherent coupling between two optical probes and to beat the SQL [29,40]. The difference is that the nonlinear crystal is not needed in our case, resulting in the parametric interaction. A nonlinear coherent coupling between the modes is achieved via the ponderomotive nonlinearity of the movable mirror. Importantly, two optical outputs are used in the scheme described in our paper, while a single output was utilized in Refs. [29,40].

A. Main assumptions

Let us consider the scheme shown in Fig. 2. We assume that the relaxation rates of the eigenmodes are identical and characterized with the full width at half maximum equal to 2γ . The mechanical relaxation rate is small if compared with the optical one: $\gamma_m \ll \gamma$. We also assume that the conditions of the resolved sideband interaction and the frequency synchronization are valid:

$$\gamma_m \ll \gamma \ll \omega_m, \quad \omega_+ - \omega_- = \omega_m. \quad (2.2)$$

The resonance curves shown in Fig. 2(b) illustrate the conditions accepted above.

For the sake of simplicity we also assume that following conditions are valid:

$$L_1 \simeq L_2, \quad L_1, L_2 \gg \ell_1, \ell_2. \quad (2.3)$$

In order to perform the measurements in our system the classical resonant mechanical oscillations have to be suppressed. This can be done by using four, not two, modes

with orthogonal polarizations and optimally selected powers. It is also possible to suppress the classical oscillation via an electronic feedback. For the sake of simplicity we consider the simplified Hamiltonian with only two modes, assuming that the classical portion of the mechanical oscillation is suppressed by other classical means. The full analysis of the four-mode scheme confirming the assumption is given in Appendix B.

B. Hamiltonian

The generalized Hamiltonian describing the system can be presented in the following form:

$$H = H_0 + H_{\text{int}} + H_T + H_{\gamma} + H_{T,m} + H_{\gamma_m}, \quad (2.4a)$$

$$H_0 = \hbar\omega_+c_+^{\dagger}c_+ + \hbar\omega_-c_-^{\dagger}c_- + \hbar\omega_md^{\dagger}d, \quad (2.4b)$$

$$H_{\text{int}} = \frac{\hbar}{i}(\eta c_+^{\dagger}c_-d - \eta^*c_+c_-^{\dagger}d^{\dagger}). \quad (2.4c)$$

H_{int} is the Hamiltonian of the interaction between modes, d and d^{\dagger} are annihilation and creation operators of the mechanical oscillator, c_{\pm} and c_{\pm}^{\dagger} are annihilation and creation operators of the corresponding optical modes. The operator of coordinate x of the mechanical oscillator can be presented in the form

$$x = x_0(d + d^{\dagger}), \quad x_0 = \sqrt{\frac{\hbar}{2m\omega_m}}. \quad (2.5)$$

The coupling constant η can be written as

$$|\eta| \simeq \frac{x_0}{L}\omega_0, \quad L \simeq L_1, L_2, \quad \omega_0 \simeq \omega_{\pm}. \quad (2.6)$$

H_T is the Hamiltonian describing the environment (thermal bath) and H_{γ} is the Hamiltonian of the coupling between the environment and the optical modes resulting in the decay rate γ . Similarly, $H_{T,m}$ is the Hamiltonian of the environment and H_{γ_m} is the Hamiltonian describing the coupling between the environment and the mechanical oscillator resulting in the decay rate γ_m . See Appendix C for details.

It is convenient to separate the expectation values of the wave amplitudes as well as their fluctuation parts and assume that the fluctuations are small:

$$A_{\pm} = (A_{\pm} + \hat{a}_{\pm})e^{-i\omega_{\pm}t}, \quad (2.7)$$

$$B_{\pm} = (B_{\pm} + \hat{b}_{\pm})e^{-i\omega_{\pm}t}. \quad (2.8)$$

A_{\pm} and B_{\pm} stand for the expectation values of the amplitudes of the corresponding optical waves and a_{\pm} and b_{\pm} represent the fluctuations, $|A_{\pm}|^2 \gg \langle a_{\pm}^{\dagger}a_{\pm} \rangle$ and $|B_{\pm}|^2 \gg \langle b_{\pm}^{\dagger}b_{\pm} \rangle$, where $\langle \dots \rangle$ stands for ensemble averaging.

The normalization of the amplitudes is selected so that $\hbar\omega_{\pm}|A_{\pm}|^2$ describes the optical power [28]. We also consider only spectral components around carrier frequencies ω_{\pm} and drop the harmonics centered at frequencies $(\omega_+ + \omega_m)$ and $(\omega_- - \omega_m)$ far from the corresponding resonances.

The Hamiltonian of the system allows us to write the equations of motion for the intracavity fields:

$$\hat{c}_+ + \gamma\hat{c}_+ + \eta c_- \hat{d} = \sqrt{2\gamma}\hat{a}_+, \quad (2.9a)$$

$$\hat{c}_- + \gamma\hat{c}_- - \eta c_+ \hat{d}^{\dagger} = \sqrt{2\gamma}\hat{a}_-. \quad (2.9b)$$

The complete derivation of these equations is presented in Appendix C.

The input-output relations are

$$\hat{b}_{\pm} = -\hat{a}_{\pm} + \sqrt{2\gamma}\hat{c}_{\pm}. \quad (2.9c)$$

III. SOLUTION

Using the Hamiltonian formalism we obtain the following set of equations for the expectation values:

$$\gamma C_+ + \eta C_- D = \sqrt{2\gamma}A_+, \quad (3.1a)$$

$$\gamma C_- - \eta^* C_+ D^* = \sqrt{2\gamma}A_-, \quad (3.1b)$$

$$\gamma_m D = \eta^* C_+ C_-^*, \quad (3.1c)$$

$$\gamma_m D^* = \eta C_+^* C_-. \quad (3.1d)$$

Introducing the parameter $\nu = |\eta|^2/\gamma\gamma_m$, we arrive at

$$C_+ \left(1 + \frac{\nu g^2 |A_-|^2}{(1 - \nu |C_+|^2)^2} \right) = \sqrt{\frac{2}{\gamma}} A_+, \quad (3.2a)$$

$$C_- \left(1 - \frac{\nu g^2 |A_+|^2}{(1 + \nu |C_-|^2)^2} \right) = \sqrt{\frac{2}{\gamma}} A_-. \quad (3.2b)$$

The amplitudes C_+ and C_- are limited due to the ponderomotive nonlinearity. The classical resonant ponderomotive force creates mechanical oscillations with the amplitude D which can be large. These oscillations are classical and can be suppressed using a regular force optimized for the known amplitudes of the probe fields. We also can use two orthogonal polarizations in the scheme shown in Fig. 2 to reduce the undesirable resonant excitation of the mechanical oscillator (see Appendix B for details). In what follows we omit them from consideration and assume that $D = 0$ and $C_{\pm} = \sqrt{2/\gamma}A_{\pm}$.

A. Langevin equations

The equations of motion for the Fourier amplitudes of the operators describing the intracavity fields and the mechanical oscillator, c_{\pm} and d , can be written in the following forms using (2.9a) and (2.9b):

$$(\gamma - i\Omega)c_+(\Omega) + \eta C_- d(\Omega) = \sqrt{2\gamma}a_+(\Omega), \quad (3.3a)$$

$$(\gamma - i\Omega)c_-(\Omega) - \eta^* C_+ d^\dagger(-\Omega) = \sqrt{2\gamma}a_-(\Omega), \quad (3.3b)$$

$$\begin{aligned} (\gamma_m - i\Omega)d(\Omega) - \eta^* [C_-^* c_+(\Omega) + C_+ c_-^\dagger(-\Omega)] \\ = \sqrt{2\gamma_m} q(\Omega) + i f_s(\Omega), \end{aligned} \quad (3.3c)$$

$$b_{\pm}(\Omega) = -a_{\pm}(\Omega) + \sqrt{2\gamma} c_{\pm}(\Omega), \quad (3.3d)$$

where b_{\pm} are the output Fourier amplitudes of the optical waves. The incident waves are in the coherent state, so the operators \hat{a}_{\pm} are characterized with the following commutators and correlators:

$$[\hat{a}_{\pm}(t), \hat{a}_{\pm}^\dagger(t')] = \delta(t - t'), \quad (3.4)$$

$$\langle \hat{a}_{\pm}(t) \hat{a}_{\pm}^\dagger(t') \rangle = \delta(t - t'), \quad (3.5)$$

where $\langle \dots \rangle$ stands for ensemble averaging.

The Fourier transforms of these operators are introduced as follows:

$$\hat{a}_{\pm}(t) = \int_{-\infty}^{\infty} a_{\pm}(\Omega) e^{-i\Omega t} \frac{d\Omega}{2\pi}. \quad (3.6)$$

The same is true for the other operators. Using (3.4) and (3.5) we derive commutators and correlators for the Fourier amplitudes of the input fluctuation operators as follows:

$$[a_{\pm}(\Omega), a_{\pm}^\dagger(\Omega')] = 2\pi \delta(\Omega - \Omega'), \quad (3.7)$$

$$\langle a_{\pm}(\Omega) a_{\pm}^\dagger(\Omega') \rangle = 2\pi \delta(\Omega - \Omega'). \quad (3.8)$$

For the signal force we also introduce its Fourier amplitude assuming that the force is the resonant one acting during the time interval τ :

$$\begin{aligned} F_s(t) &= F_{s0} \cos(\omega_m t + \psi_f) \\ &= F_s(t) e^{-i\omega_m t} + F_s^*(t) e^{i\omega_m t}, \quad -\frac{\tau}{2} < t < \frac{\tau}{2}, \end{aligned} \quad (3.9)$$

$$f_s(\Omega) = \frac{F_s(\Omega)}{\sqrt{2\hbar\omega_m m}}, \quad f_{s0} = \frac{F_{s0}(\Omega)}{\sqrt{2\hbar\omega_m m}} = 2f_s, \quad (3.10)$$

where $F_s(\Omega)$ is the Fourier amplitude of the slow complex amplitude $F_s(t)$. In the general case, $F_s(\Omega) \neq F_s^*(-\Omega)$.

The thermal mechanical noise operators are described using the following expressions:

$$[q(\Omega), q^\dagger(\Omega')] = 2\pi \delta(\Omega - \Omega'), \quad (3.11a)$$

$$\langle q(\Omega) q^\dagger(\Omega') \rangle = (2n_T + 1) 2\pi \delta(\Omega - \Omega'), \quad (3.11b)$$

$$n_T = \frac{1}{e^{\hbar\omega_m/\kappa_B T} - 1}. \quad (3.11c)$$

Here κ_B is the Boltzmann constant, and T is the ambient temperature.

It is important to note that the optical modes contain information on the mechanical oscillator in a slightly different way. The annihilation operator $\sim d$ impacts c_+ in (3.3a) and the creation operator $\sim d^\dagger$ impacts c_- in (3.3b). This is usual for parametric processes and is essential for the measurement procedure described below.

B. Solution of the Langevin equations

For the sake of simplicity we assume that the phases of the probe harmonics are selected so that

$$C_+ = C_+^* = C_- = C_-^* = C, \quad \eta = \eta^*. \quad (3.12)$$

Introducing the quadrature amplitudes

$$a_{\pm a} = \frac{a_{\pm}(\Omega) + a_{\pm}^\dagger(-\Omega)}{\sqrt{2}}, \quad (3.13a)$$

$$a_{\pm \phi} = \frac{a_{\pm}(\Omega) - a_{\pm}^\dagger(-\Omega)}{i\sqrt{2}}, \quad (3.13b)$$

and using (3.3), we obtain

$$(\gamma - i\Omega)c_{+a} + \eta C d_a = \sqrt{2\gamma}a_{+a}, \quad (3.14a)$$

$$(\gamma - i\Omega)c_{+\phi} + \eta C d_\phi = \sqrt{2\gamma}a_{+\phi}, \quad (3.14b)$$

$$(\gamma - i\Omega)c_{-a} - \eta C d_a = \sqrt{2\gamma}a_{-a}, \quad (3.14c)$$

$$(\gamma - i\Omega)c_{-\phi} + \eta C d_\phi = \sqrt{2\gamma}a_{-\phi}, \quad (3.14d)$$

$$(\gamma_m - i\Omega)d_a - \eta C(c_{+a} + c_{-a}) = \sqrt{2\gamma_m}q_a - f_{s\phi}, \quad (3.14e)$$

$$(\gamma_m - i\Omega)d_\phi - \eta C(c_{+\phi} - c_{-\phi}) = \sqrt{2\gamma_m}q_\phi + f_{s\phi}. \quad (3.14f)$$

The sum of amplitude quadratures, $c_{+a} + c_{-a}$, on one hand, does not contain information on the mechanical motion (the term proportional to $\sim d_a$ is absent), and, on the other hand, produces the backaction term in Eq. (3.14e). The difference of phase quadratures, $c_{+\phi} - c_{-\phi}$, does not contain d_ϕ but produces backaction in Eq. (3.14f). We use this feature to achieve the backaction evasion in the force detection.

We would like to stress here that in the measurement scheme illustrated in Fig. 2 one can measure any single quadrature independently in each frequency and spatial channel separated from the other channels. The results of the measurements can be combined and processed after the measurement is done. For example, one can detect amplitude quadratures b_{+a} and b_{-a} and then combine their sum and difference numerically. Another possibility is to measure phase quadratures $b_{+\phi}$ and $b_{-\phi}$ and to combine their sum and difference. However, it is not allowed to measure $b_{\pm a}$ and $b_{\pm\phi}$ at the same time.

So introducing

$$g_{a\pm} = \frac{c_{+a} \pm c_{-a}}{\sqrt{2}}, \quad g_{\phi\pm} = \frac{c_{+\phi} \pm c_{-\phi}}{\sqrt{2}}, \quad (3.15)$$

$$\alpha_{a\pm} = \frac{a_{+a} \pm a_{-a}}{\sqrt{2}}, \quad \alpha_{\phi\pm} = \frac{a_{+\phi} \pm a_{-\phi}}{\sqrt{2}}, \quad (3.16)$$

$$\beta_{a\pm} = \frac{b_{+a} \pm b_{-a}}{\sqrt{2}}, \quad \beta_{\phi\pm} = \frac{b_{+\phi} \pm b_{-\phi}}{\sqrt{2}}, \quad (3.17)$$

and rewriting (3.14) in the new notations

$$(\gamma - i\Omega)g_{a+} = \sqrt{2\gamma}\alpha_{a+}, \quad (3.18a)$$

$$(\gamma - i\Omega)g_{a-} + \sqrt{2}\eta C d_a = \sqrt{2\gamma}\alpha_{a-}, \quad (3.18b)$$

$$(\gamma_m - i\Omega)d_a - \sqrt{2}\eta C g_{a+} = \sqrt{2\gamma_m}q_a - f_{s\phi}, \quad (3.18c)$$

$$(\gamma - i\Omega)g_{\phi+} + \sqrt{2}\eta C d_\phi = \sqrt{2\gamma}\alpha_{\phi+}, \quad (3.18d)$$

$$(\gamma - i\Omega)g_{\phi-} = \sqrt{2\gamma}\alpha_{\phi-}, \quad (3.18e)$$

$$(\gamma_m - i\Omega)d_\phi - \sqrt{2}\eta C g_{\phi-} = \sqrt{2\gamma_m}q_\phi + f_{s\phi}, \quad (3.18f)$$

we find that sets [(3.18a), (3.18b), (3.18c)] and [(3.18d), (3.18e), (3.18f)] are decoupled.

It is convenient to present the solution of the set [(3.18a), (3.18b), (3.18c)] for the amplitude quadratures in the form

$$\beta_{a+} = \xi \alpha_{a+}, \quad \xi = \frac{\gamma + i\Omega}{\gamma - i\Omega}, \quad (3.19a)$$

$$\beta_{a-} = \xi \left(\alpha_{a-} - \frac{\mathcal{K} \alpha_{a+}}{\gamma_m - i\Omega} \right) - \frac{\sqrt{\xi} \mathcal{K}}{\gamma_m - i\Omega} (\sqrt{2\gamma_m}q_a - f_{s\phi}), \quad (3.19b)$$

$$\mathcal{K} \equiv \frac{4\gamma \eta^2 C^2}{\gamma^2 + \Omega^2}. \quad (3.19c)$$

As expected, in Eq. (3.19b) the backaction term is proportional to the normalized probe power \mathcal{K} . However, this term can be excluded in the postprocessing. One can measure *both* β_{a+} and β_{a-} simultaneously and subtract β_{a+} from β_{a-} to remove the backaction completely. This means that we can measure the combination as

$$\beta_{a+}^{\text{comb}} = \beta_{a-} + \xi \frac{\mathcal{K} \alpha_{a+}}{\gamma_m - i\Omega} \quad (3.20)$$

$$= \xi \alpha_{a-} - \frac{\sqrt{\xi} \mathcal{K}}{\gamma_m - i\Omega} (\sqrt{2\gamma_m}q_a - f_{s\phi}), \quad (3.21)$$

which is completely backaction free. This is the main finding of the study.

Let us write the force detection condition in terms of the single-sided power spectral density $S_f(\Omega)$ recalculated to the signal force (3.9). Demanding the signal-to-noise ratio to exceed unity, we get

$$f_{s0} \geq \sqrt{S_f(\Omega) \frac{\Delta\Omega}{2\pi}}, \quad (3.22)$$

where $\Delta\Omega \simeq 2\pi/\tau$. Using (3.8) and (3.11b), we obtain the following for the case when we measure β_{-a} (3.19b):

$$S_f(\Omega) = 2\gamma_m(2n_T + 1) + \frac{(\gamma_m^2 + \Omega^2)}{|\mathcal{K}|} + |\mathcal{K}| \geq 2\gamma_m(2n_T + 1) + S_{\text{SQL},f}, \quad (3.23)$$

$$S_{\text{SQL},f} = 2\sqrt{\gamma_m^2 + \Omega^2}. \quad (3.24)$$

The sensitivity is restricted by the SQL. If we measure β_{-a}^{comb} (3.21), the spectral density is not limited by the SQL:

$$S_f(\Omega) = 2\gamma_m(2n_T + 1) + \frac{(\gamma_m^2 + \Omega^2)}{|\mathcal{K}|}. \quad (3.25)$$

Here the first term describes the thermal noise and the last one stands for the quantum measurement noise (shot noise). The quantum measurement noise decreases with the power increase. The backaction term is absent.

It worth noting that the thermal noise term is present in any optomechanical detection scheme. It can exceed the measurement error related to the measurement apparatus rather significantly. However, a proper measurement procedure allows one to suppress this noise and also exclude the initial quantum uncertainty associated with the mechanical system. The main requirement for such a measurement is a fast interrogation time, which should be much shorter than the ringdown time of the mechanical system [12, 13]. This is possible if the measurement bandwidth exceeds the bandwidth of the mechanical mode. Sensitivity of narrowband resonant measurements is usually limited by the thermal noise.

Instead of the amplitude quadratures one can measure sums and differences of the phase quadratures. Solving the set

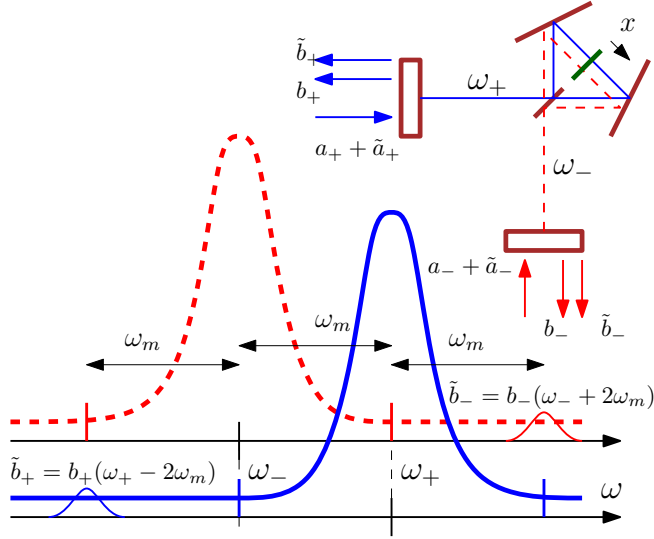


FIG. 3. Side bands $\tilde{c}_{\pm} = c_{\pm}(\omega_{\pm} \mp 2\omega_m)$ inside the cavity produce a parasitic backaction force acting on the mechanical oscillator. We assume that one can measure waves b_{\pm} and sidebands \tilde{b}_{\pm} separately.

[(3.18d), (3.18e), (3.18f)], we arrive at

$$\beta_{\phi-} = \xi \alpha_{\phi-}, \quad (3.26a)$$

$$\beta_{\phi+} = \xi \left(\alpha_{\phi+} - \frac{\mathcal{K} \alpha_{\phi-}}{\gamma_m - i\Omega} \right) - \frac{\sqrt{\xi \mathcal{K}}}{\gamma_m - i\Omega} (\sqrt{2\gamma_m} q_{\phi} + f_{sa}). \quad (3.26b)$$

We can measure quadratures $\beta_{\pm\phi}$ simultaneously and subtract the backaction proportional to $\beta_{-\phi}$ from $\beta_{+\phi}$.

Finally, a generalization is possible for a pair of quadratures with the arbitrary parameter φ :

$$b_{+\varphi} = b_{+a} \cos \varphi + b_{+\phi} \sin \varphi, \quad (3.27a)$$

$$b_{-\varphi} = b_{-a} \cos \varphi - b_{-\phi} \sin \varphi. \quad (3.27b)$$

The sum $b_{+\varphi} + b_{-\varphi}$ is not disturbed by the mechanical motion but contains the term proportional to the backaction force, whereas the difference $b_{+\varphi} - b_{-\varphi}$ contains the term proportional to the mechanical motion (with backaction and signal). The backaction term can be measured and subtracted from the force measurement result.

IV. PARASITIC BACKACTION

The fluctuation force acting on the mechanical oscillator is proportional to the cross product $(c_- c_+^\dagger + c_+^\dagger c_-)$ of the probe modes. This means that the fluctuation fields characterized by the Fourier amplitude $\tilde{c}_-(\Omega) = c_-(\omega_- + 2\omega_m + \Omega)$ centered at frequencies in the vicinity of $\omega_- + 2\omega_m$ and the Fourier amplitude $\tilde{c}_+(\Omega) = c_+(\omega_+ - 2\omega_m + \Omega)$ centered at frequencies in the vicinity of $\omega_+ - 2\omega_m$ (see Fig. 3) contribute to the ponderomotive fluctuation force impinging by the light on the mirror. We mark with a tilde these complex amplitudes of the input and output waves for the sake of shortness. We neglect these harmonics in the analysis above because the amplitude of the harmonics can be small. In what follows we

take them into account and find the limitations they introduce for the measurement strategy proposed here.

Parasitic sidebands provide additional terms to the expressions of the optical fields, for instance, Eq. (3.21) should be rewritten as

$$\beta_{a-}^{\text{comb}} = \xi \left[\alpha_{a-} + \frac{\mathcal{K} \tilde{g}_{a+}}{(\gamma_m - i\Omega)} \frac{(\gamma - i\Omega)}{\sqrt{2\gamma}} - \frac{\sqrt{\xi \mathcal{K}}}{\gamma_m - i\Omega} (\sqrt{2\gamma_m} q_a - f_{s\phi}) \right], \quad (4.1)$$

where noise term \tilde{g}_{a+} , defined by (D9), at conditions (2.2) is approximately equal to

$$\tilde{g}_{a+} \simeq \frac{\sqrt{\gamma}}{2\omega_m} [\tilde{a}_{+\phi} - \tilde{a}_{-\phi}]. \quad (4.2)$$

See Appendix D for details.

The backaction created by the parasitic sidebands limits sensitivity of the measurements. Instead of (3.23) we obtain a corrected expression for the single-sided power spectral density that can be presented as

$$S_f(\Omega) = 2\gamma_m(2n_T + 1) + \frac{(\gamma_m^2 + \Omega^2)}{|\mathcal{K}|} + \frac{|\mathcal{K}|(\gamma^2 + \Omega^2)}{4\omega_m^2} \geq 2\gamma_m(2n_T + 1) + \frac{\sqrt{\gamma^2 + \Omega^2}}{2\omega_m} S_{\text{SQL},f} \quad (4.3)$$

While the sensitivity still can be less than the SQL at conditions (2.2), the sensitivity becomes limited after the probe power reaches the optimal value found from Eq. (4.3):

$$|\mathcal{K}|^2 = 4\omega_m^2 \frac{\gamma_m^2 + \Omega^2}{\gamma^2 + \Omega^2} \gg |\mathcal{K}_{\text{SQL}}|^2, \quad (4.4)$$

where \mathcal{K}_{SQL} corresponds to the optimal power value needed to reach the SQL in the system.

The impact of the parasitic harmonics can be reduced if one is able to measure $\tilde{b}_-(\Omega) = b_-(\omega_- + 2\omega_m + \Omega)$ as well as $\tilde{b}_+(\Omega) = b_+(\omega_+ - 2\omega_m + \Omega)$ independently on the other spectral components of the output light. The measurement can be performed if narrowband bandpass filters are available.

The scheme of such a measurement is illustrated in Fig. 3. Measurement of optimally selected quadratures of \tilde{b}_{\pm} allows partial reduction of the parasitic backaction described by the term \tilde{g}_{a+} in Eq. (4.1). The reduction factor is $R \simeq \Omega/2\omega_m \ll 1$ (see details in Appendix E).

This means that, in the case $\gamma_m = 0$ and at conditions (2.2), the formula (4.3) will have the form

$$S_f(\Omega) = \frac{\Omega^2}{|\mathcal{K}|} + \frac{|\mathcal{K}| \gamma^2 \Omega^2}{16\omega_m^4} \geq \frac{\gamma |\Omega|}{2\omega_m^2} S_{\text{SQL},f}. \quad (4.5)$$

The sensitivity (4.5) is better than that defined by Eq. (4.3) achieved for the case of not suppressed parasitic harmonics.

V. DISCUSSION AND CONCLUSION

In the transducers shown in Figs. 1 and 2, the information on the mechanical *quadratures* transfers to the optical quadratures of two independent probe fields which can be measured *independently*. It provides an alternative possibility

TABLE I. Proposed set of optomechanical parameters.

Parameter	Value
Mechanical oscillator frequency $\omega_m/2\pi$	2.5 MHz
Mechanical rate of decay $\gamma_m/2\pi$	100 Hz
Oscillator mass m	10 ng
Cavity length L	40 cm
Pump frequency $\omega_0/2\pi$	300 THz
Optical rate of decay $\gamma/2\pi$	0.1 MHz

of postprocessing analysis leading to the broadband backaction evasion.

For example, one can measure amplitude quadrature components in each output, save them, and then combine them numerically, taking their sum and difference. This gives the unique possibility to (a) record the backaction force without any information on mechanical displacement (in the sum of quadratures) and (b) record the position of the oscillator with shot noise and backaction. Then one can subtract the backaction completely using the recorded data. At this stage the quantum fluctuations are already reduced to the classical numbers.

One also can measure phase quadrature amplitudes independently in both outputs and combine their sum and difference. In this case the difference contains pure backaction force and the sum includes information about the position of the mechanical oscillator with shot noise and backaction, as shown by Eq. (3.14). This is a peculiar property of the parametric interaction. In this case the backaction can be subtracted completely.

One of the main features of the measurement strategy proposed here is in the usage of the dichromatic probe field that results in the two independent quantum outputs. It gives us the flexibility to measure the backaction separately and then subtract it completely from the measurement result. The subtraction can be made in a broad frequency band.

In contrast, in conventional variational measurements [26–28] there is only one quantum output and the backaction cannot be measured separately from the signal. Measurement of the linear combination of the amplitude and phase quadratures in that case allows partial subtraction of the backaction. Only one quadrature of the output wave has to be measured to surpass the SQL.

The single-channel measurement of the optical quadrature is a common feature in many practical schemes of backaction evasion force detection, including the optical spring [16–18], ancilla cavity and parametric amplification [29,40], and the nonclassical probe [19–25]; all of these result in backaction evasion measurements. In all these schemes only one quantum output is generally utilized.

The scheme proposed here allows measurement of either a combination of a sum and a difference of amplitude quadratures (3.21) or a sum and a difference of phase quadratures (3.26) of two optical probe harmonics. Generalization (3.27) is also possible. These measurement strategies lead to backaction evasion in a broad frequency band. We expect that this technique will find a realization in other metrological configurations.

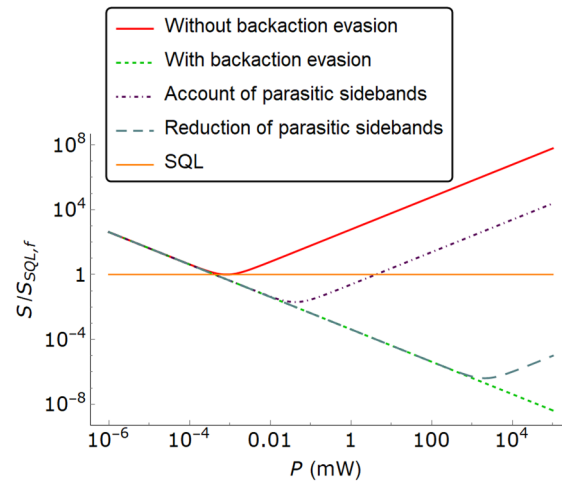


FIG. 4. Noise power spectral densities S as a function of the input power P . Measurement of only β_{-a} (red line) (3.23) does not allow the SQL to be surpassed (horizontal orange line) (3.24). Measurement of the combination β_a^{comb} (dashed green line) (3.25) allows backaction to be evaded and the SQL to be surpassed. It is still possible to surpass the SQL with parasitic harmonics taken into account (dot-dashed purple line) (4.3) but the corresponding Power spectral density (PSD) rises at higher pump-power levels. Reduction of parasitic harmonics (blue line) (4.5) improves sensitivity but the corresponding PSD still rises at higher pump-power levels. The plots are presented for $\Omega/2\pi = 100$ Hz. The parameters used for the plots' evaluation are given in Table I except for $\gamma_m = 0$.

It is important to know precise values of the system parameters to realize the proposed technique experimentally. There are techniques for identification of those parameters [18]. To illustrate numerically the expected performance of the system described here we have introduced realistic numerical parameters listed in Table I and evaluated the power spectral density of the measurement noise (Fig. 4). The values of these parameters are based on estimations and assumptions given in Refs. [18,45]. The plots are presented for the ideal case of $\gamma_m = 0$ and $n_r = 0$ which corresponds to solely quantum noise without thermal noise. Crystalline strained silicon seems to be a promising material because mechanical nanooscillators made of it have quality factor $Q > 10^{10}$ [46], which is ten times higher than the quality factor of oscillators made of Si_3N_4 [47].

We propose to use filtration of output waves in order to depress backaction due to parasitic sidebands. Experimental realization of this filtration is not a simple task, but it is possible *in principle*.

ACKNOWLEDGMENTS

The research of S.P.V. and A.I.N. has been supported by the Russian Foundation for Basic Research (Grant No. 19-29-11003), the Interdisciplinary Scientific and Educational School of Moscow University “Fundamental and Applied Space Research” and the TAPIR GIFT MSU Support of the California Institute of Technology. A.I.N. is the recipient of a Theoretical Physics and Mathematics Advancement Foundation “BASIS” scholarship (Contract No. 20-2-1-96-1). The

research reported here performed by A.B.M. was carried out at the Jet Propulsion Laboratory, California Institute of Technology, under a contract with the National Aeronautics and Space Administration (Contract No. 80NM0018D0004). This document has LIGO No. P2100139.

APPENDIX A: HAMILTONIAN FOR SCHEME IN FIG. 1

Here we derived the Hamiltonian for the scheme in Fig. 1 in order to demonstrate that it is similar to Hamiltonian (2.4).

We consider clockwise and counterclockwise modes with amplitudes c_1 and c_2 coupled with each other by a small coupling coefficient κ (2.1), assuming that its phase φ is $\phi = \phi_0 + 2kx$. We write the cavity Hamiltonian as follows:

$$H = H_0 + H_{\text{int}} + H_m, \quad (\text{A1a})$$

$$H_0 = \hbar\omega(c_1^\dagger c_1 + c_2^\dagger c_2), \quad H_m = \hbar\omega_m d^\dagger d, \quad (\text{A1b})$$

$$H_{\text{int}} = \frac{\hbar}{i}(\kappa c_1^\dagger c_2 - \kappa^* c_1 c_2^\dagger). \quad (\text{A1c})$$

Let us introduce eigenmodes c_p and c_m inside the cavity

$$\kappa_0 = |\kappa_0|e^{i\phi}, \quad \phi = \phi_0 + 2kx, \quad (\text{A2a})$$

$$c_{p,m} = \frac{c_1 \pm ic_2 e^{2i\phi_0}}{\sqrt{2}} \quad (\text{A2b})$$

and express the optical part of Hamiltonian (A.1) (without H_m) as

$$\begin{aligned} H &= \hbar\omega(c_p^\dagger c_p + c_m^\dagger c_m) + \hbar|\kappa|(c_m^\dagger c_m - c_p^\dagger c_p) \cos 2kx \\ &\quad - \frac{\hbar|\kappa|}{i}[c_m^\dagger c_p - c_p^\dagger c_m] \sin 2kx \\ &\simeq \hbar(\omega - |\kappa|)c_p^\dagger c_p + \hbar(\omega + |\kappa|)c_m^\dagger c_m \\ &\quad - \frac{\hbar|\kappa|}{i}[c_p^\dagger c_m - c_m^\dagger c_p]2kx. \end{aligned} \quad (\text{A3a})$$

Here k is the optical wave vector, x is displacement of mirror M , and we assume $kx \ll 1$.

Using the rotating-wave approximation and notation (2.5), we reduce Hamiltonian (A3) to Hamiltonian (2.4).

APPENDIX B: SUPPRESSION OF THE RESONANT PONDEROMOTIVE EXCITATION

In this section we discuss possibilities of the suppression of resonant ponderomotive excitation of the mechanical oscillations of the system.

We assume that there exist modes c_+ and e_+ characterized by orthogonal polarizations and the same geometrical path. These modes are characterized by the eigenfrequency ω_+ . Similarly, modes c_- and e_- are characterized by orthogonal polarizations and the same eigenfrequency ω_- . In this configuration (2.4),

$$H = \tilde{H}_0 + \tilde{H}_{\text{int}} + \tilde{H}_\gamma, \quad (\text{B1a})$$

$$\begin{aligned} \tilde{H}_0 &= \hbar\omega_+ c_+^\dagger c_+ + \hbar\omega_- c_-^\dagger c_- + \hbar\omega_+ e_+^\dagger e_+ \\ &\quad + \hbar\omega_- e_-^\dagger e_- + \hbar\omega_m d^\dagger d, \end{aligned} \quad (\text{B1b})$$

$$\begin{aligned} \tilde{H}_{\text{int}} &= \frac{\hbar}{i}(\eta c_+^\dagger c_- d - \eta^* c_+ c_-^\dagger d^\dagger) + \frac{\hbar}{i}(\eta_e e_+^\dagger e_- d - \eta_e^* e_+ e_-^\dagger d^\dagger). \end{aligned} \quad (\text{B1c})$$

From this Hamiltonian we derive the equations of motion for the intracavity fields:

$$\dot{c}_+ + \gamma c_+ + \eta c_- d = \sqrt{2\gamma} a_+, \quad (\text{B2a})$$

$$\dot{c}_- + \gamma c_- - \eta^* c_+ d^\dagger = \sqrt{2\gamma} a_-, \quad (\text{B2b})$$

$$\dot{e}_+ + \gamma e_+ + \eta_e e_- d = \sqrt{2\gamma} a_+^e, \quad (\text{B2c})$$

$$\dot{e}_- + \gamma e_- - \eta_e^* e_+ d^\dagger = \sqrt{2\gamma} a_-^e, \quad (\text{B2d})$$

$$\dot{d} + \gamma_m d = \eta^* c_+ c_-^\dagger + \eta_e^* e_+ e_-^\dagger + \sqrt{2\gamma} q + if_s. \quad (\text{B2e})$$

The input-output relations are given as

$$b_\pm = -a_\pm + \sqrt{2\gamma} c_\pm, \quad b_\pm^e = -a_\pm^e + \sqrt{2\gamma} e_\pm. \quad (\text{B3a})$$

Here a_\pm and b_\pm are the input and output fields of the c_\pm modes, and a_\pm^e and b_\pm^e are the input and output fields of the e_\pm modes. Equations for the mean amplitudes follow from (B2):

$$\gamma C_+ + \eta C_- D = \sqrt{2\gamma} A_+, \quad (\text{B4a})$$

$$\gamma C_- - \eta^* C_+ D^* = \sqrt{2\gamma} A_-, \quad (\text{B4b})$$

$$\gamma E_+ + \eta_e E_- D = \sqrt{2\gamma} A_+^e, \quad (\text{B4c})$$

$$\gamma E_- - \eta_e^* E_+ D^* = \sqrt{2\gamma} A_-^e, \quad (\text{B4d})$$

$$\gamma_m D = \eta^* C_+ C_-^* + \eta_e^* E_+ E_-^*. \quad (\text{B4e})$$

We consider the case of equal coupling constants $\eta = \eta_e$. For the sake of simplicity we choose

$$\eta = \eta^* = \eta_e = \eta_e^*, \quad (\text{B5a})$$

$$C_+ = C_- = C = C^*. \quad (\text{B5b})$$

In order to suppress the mean amplitude of the mechanical oscillator we have to pump e_\pm modes so

$$E_+ = E_-^* = -iC \text{ (or } iC). \quad (\text{B6})$$

Then we get the following equations for the fluctuation parts:

$$(\gamma - i\Omega)c_+ + \eta Cd = \sqrt{2\gamma} a_+, \quad (\text{B7a})$$

$$(\gamma - i\Omega)c_- - \eta Cd^\dagger = \sqrt{2\gamma} a_-, \quad (\text{B7b})$$

$$(\gamma - i\Omega)e_+ + i\eta Cd = \sqrt{2\gamma} a_+^e, \quad (\text{B7c})$$

$$(\gamma - i\Omega)e_- + i\eta Cd^\dagger = \sqrt{2\gamma} a_-^e, \quad (\text{B7d})$$

$$(\gamma_m - i\Omega)d = \eta C(c_+ + c_-^\dagger) - i\eta C(e_+ + e_-^\dagger). \quad (\text{B7e})$$

Introducing quadrature amplitudes as in (3.13), we obtain

$$(\gamma - i\Omega)c_{+\phi} + \eta Cd_a = \sqrt{2\gamma} a_{+\phi}, \quad (\text{B8a})$$

$$(\gamma - i\Omega)c_{+\phi} + \eta Cd_\phi = \sqrt{2\gamma} a_{+\phi}, \quad (\text{B8b})$$

$$(\gamma - i\Omega)c_{-\phi} - \eta Cd_a = \sqrt{2\gamma} a_{-\phi}, \quad (\text{B8c})$$

$$(\gamma - i\Omega)c_{-\phi} + \eta Cd_\phi = \sqrt{2\gamma} a_{-\phi}, \quad (\text{B8d})$$

$$(\gamma - i\Omega)e_{+\phi} - \eta Cd_\phi = \sqrt{2\gamma} a_{+\phi}^e, \quad (\text{B8e})$$

$$(\gamma - i\Omega)e_{+\phi} + \eta Cd_a = \sqrt{2\gamma} a_{+\phi}^e, \quad (\text{B8f})$$

$$(\gamma - i\Omega)e_{-\phi} - \eta Cd_\phi = \sqrt{2\gamma} a_{-\phi}^e, \quad (\text{B8g})$$

$$(\gamma - i\Omega)e_{-\phi} + \eta Cd_a = \sqrt{2\gamma} a_{-\phi}^e, \quad (\text{B8h})$$

$$(\gamma_m - i\Omega)d_a - \eta C(c_{+a} + c_{-a} + e_{+\phi} - e_{-\phi}) = \sqrt{2\gamma_m}q_a - f_{s\phi}, \quad (\text{B8i})$$

$$(\gamma_m - i\Omega)d_\phi - \eta C(c_{+\phi} - c_{-\phi} - e_{+a} - e_{-a}) = \sqrt{2\gamma_m}q_\phi + f_{sa}. \quad (\text{B8j})$$

Then we combine amplitudes as in (3.15), (3.16), and (3.17):

$$\epsilon_{a\pm} = \frac{e_{+a} \pm e_{-a}}{\sqrt{2}}, \quad \epsilon_{\phi\pm} = \frac{e_{+\phi} \pm e_{-\phi}}{\sqrt{2}}, \quad (\text{B9a})$$

$$\alpha_{a\pm}^e = \frac{a_{+a}^e \pm a_{-a}^e}{\sqrt{2}}, \quad \alpha_{\phi\pm}^e = \frac{a_{+\phi}^e \pm a_{-\phi}^e}{\sqrt{2}}, \quad (\text{B9b})$$

$$\beta_{a\pm}^e = \frac{b_{+a}^e \pm b_{-a}^e}{\sqrt{2}}, \quad \beta_{\phi\pm}^e = \frac{b_{+\phi}^e \pm b_{-\phi}^e}{\sqrt{2}}, \quad (\text{B9c})$$

and we rewrite (B8) using these combinations, similarly to (3.18):

$$(\gamma - i\Omega)g_{a+} = \sqrt{2\gamma}\alpha_{a+}, \quad (\text{B10a})$$

$$(\gamma - i\Omega)g_{a-} + \sqrt{2\eta}Cd_a = \sqrt{2\gamma}\alpha_{a-}, \quad (\text{B10b})$$

$$(\gamma - i\Omega)\epsilon_{\phi+} + \sqrt{2\eta}Cd_a = \sqrt{2\gamma}\alpha_{\phi+}^e, \quad (\text{B10c})$$

$$(\gamma - i\Omega)\epsilon_{\phi-} = \sqrt{2\gamma}\alpha_{\phi-}^e, \quad (\text{B10d})$$

$$(\gamma_m - i\Omega)d_a - \sqrt{2\eta}C(g_{a+} + \epsilon_{\phi-}) = \sqrt{2\gamma_m}q_a - f_{s\phi}, \quad (\text{B10e})$$

$$(\gamma - i\Omega)g_{\phi+} + \sqrt{2\eta}Cd_\phi = \sqrt{2\gamma}\alpha_{\phi+}, \quad (\text{B10f})$$

$$(\gamma - i\Omega)g_{-\phi} = \sqrt{2\gamma}\alpha_{\phi-}, \quad (\text{B10g})$$

$$(\gamma - i\Omega)\epsilon_{a+} = \sqrt{2\gamma}\alpha_{a+}^e, \quad (\text{B10h})$$

$$(\gamma - i\Omega)\epsilon_{a-} - \sqrt{2\eta}Cd_\phi = \sqrt{2\gamma}\alpha_{a-}^e, \quad (\text{B10i})$$

$$(\gamma_m - i\Omega)d_\phi - \sqrt{2\eta}C(g_{\phi-} - \epsilon_{a+}) = \sqrt{2\gamma_m}q_\phi + f_{sa}. \quad (\text{B10j})$$

So, in order to completely evade backaction from modes c and e as it follows from (B10e) we have to measure simultaneously the next combination of output quadratures:

$$\beta_{a-}^{\text{comb}} = \beta_{a-} + \frac{\mathcal{K}}{\gamma_m - i\Omega}(\beta_{+a} + \beta_{\phi-}^e), \quad (\text{B11a})$$

or as follows from Eq. (B10j),

$$\beta_{\phi+}^{\text{comb}} = \beta_{\phi+} + \frac{\mathcal{K}}{\gamma_m - i\Omega}(\beta_{\phi-} - \beta_{a+}^e). \quad (\text{B11b})$$

Another possibility to suppress the mechanical oscillator is having a small coupling constant η_e ($\eta_e \ll \eta$). It can be realized by engineering coating of the mirror M in Fig. 2. The larger pumps E_\pm can compensate regular force in (B4e), without introducing significant backaction noise.

APPENDIX C: DERIVATION OF THE INTRACAVITY FIELDS

Here we provide details of calculation of intracavity fields (for example, see Ref. [48]).

We begin with Hamiltonian (2.4):

$$H = H_0 + H_{\text{int}} + H_T + H_\gamma + H_{T,m} + H_{\gamma_m}, \quad (\text{C1})$$

$$H_T = \sum_{k=0}^{\infty} \hbar\omega_k b_k^\dagger b_k, \quad (\text{C2})$$

$$H_\gamma = i\hbar\sqrt{\frac{\gamma\Delta\omega}{\pi}} \sum_{k=0}^{\infty} [(c_+^\dagger + c_-^\dagger)b_k - (c_+ + c_-)b_k^\dagger], \quad (\text{C3})$$

$$H_{T,m} = \sum_{k=0}^{\infty} \hbar\omega_k q_k^\dagger q_k, \quad (\text{C4})$$

$$H_{\gamma_m} = i\hbar\sqrt{\frac{\gamma\Delta\omega}{\pi}} \sum_{k=0}^{\infty} [d^\dagger q_k - dq_k^\dagger]. \quad (\text{C5})$$

Here H_T is the Hamiltonian of the environment presented as a bath of oscillators described with frequencies $\omega_k = \omega_{k-1} + \Delta\omega$ and annihilation and creation operators b_k and b_k^\dagger . H_γ is the Hamiltonian of coupling between the environment and the optical resonator, and γ is the coupling constant. Similarly $H_{T,m}$ is the Hamiltonian of the environment presented by a thermal bath of mechanical oscillators with frequencies $\omega_k = \omega_{k-1} + \Delta\omega$ and amplitudes described with annihilation and creation operators q_k and q_k^\dagger . H_{γ_m} is the Hamiltonian of coupling between the environment and the mechanical oscillator, and $2\gamma_m$ is the decay rate of the oscillator.

We write the following Heisenberg equations for operators c_+ and b_k :

$$i\hbar\dot{c}_+ = [c_+, H] = \hbar\omega_+ c_+ - i\hbar\eta c_- d + i\hbar\sqrt{\frac{\gamma\Delta\omega}{\pi}} \sum_{k=0}^{\infty} b_k, \quad (\text{C6a})$$

$$i\hbar\dot{b}_k = [b_k, H] = \hbar\omega_k b_k - i\hbar\sqrt{\frac{\gamma\Delta\omega}{\pi}} (c_+ + c_-). \quad (\text{C6b})$$

We introduce slow amplitudes $c_\pm \rightarrow c_\pm e^{-i\omega_\pm t}$, $d \rightarrow d e^{-i(\omega_+ - \omega_-)t}$, and $b_k \rightarrow b_k e^{-i\omega_k t}$ and substitute them into (C6):

$$\dot{c}_+ = -\eta c_- d + \sqrt{\frac{\gamma\Delta\omega}{\pi}} \sum_{k=0}^{\infty} b_k e^{-i(\omega_k - \omega_+)t}, \quad (\text{C7a})$$

$$\dot{b}_k = -\sqrt{\frac{\gamma\Delta\omega}{\pi}} (c_+ e^{-i(\omega_+ - \omega_k)t} + c_- e^{-i(\omega_- - \omega_k)t}). \quad (\text{C7b})$$

Using the initial condition $b_k(t=0) = b_k(0)$ to integrate (C7b), we obtain

$$b_k(t) = b_k(0) - \int_0^t \sqrt{\frac{\gamma\Delta\omega}{\pi}} c_+(s) e^{-i(\omega_+ - \omega_k)s} ds - \int_0^t \sqrt{\frac{\gamma\Delta\omega}{\pi}} c_-(s) e^{-i(\omega_- - \omega_k)s} ds. \quad (\text{C8})$$

Using the final condition $b_k(t=\infty) = b_k(\infty)$ to integrate (C7b), we derive

$$b_k(t) = b_k(\infty) + \int_t^\infty \sqrt{\frac{\gamma\Delta\omega}{\pi}} c_+(s) e^{-i(\omega_+ - \omega_k)s} ds + \int_t^\infty \sqrt{\frac{\gamma\Delta\omega}{\pi}} c_-(s) e^{-i(\omega_- - \omega_k)s} ds. \quad (\text{C9})$$

To get the input-output relation we substitute the initial condition (C8) into (C7a),

$$\begin{aligned} \dot{c}_+ &= -\eta c_- d + \sum_{k=0}^{\infty} \sqrt{\frac{\gamma \Delta \omega}{\pi}} b_k(0) e^{-i(\omega_k - \omega_+)t} \\ &\quad - \sum_{k=0}^{\infty} \int_0^t \frac{\gamma \Delta \omega}{\pi} c_+(s) e^{-i(\omega_k - \omega_+)(t-s)} ds \\ &\quad - \left(\sum_{k=0}^{\infty} \int_0^t \frac{\gamma \Delta \omega}{\pi} c_-(s) e^{-i(\omega_k - \omega_-)(t-s)} ds \right) e^{i(\omega_+ - \omega_-)t}, \end{aligned} \quad (\text{C10})$$

omit the last term proportional to $e^{i(\omega_+ - \omega_-)t}$ as fast oscillating, and define the input field as

$$a_+(t) = \sum_{k=0}^{\infty} \sqrt{\frac{\Delta \omega}{2\pi}} b_k(0) e^{-i(\omega_k - \omega_+)t}. \quad (\text{C11})$$

To calculate the remaining sum in Eq. (C10) we assume the limit $\Delta \omega \rightarrow 0$ and replace the sum by the integral using the rule

$$\Delta \omega \sum_{k=0}^{\infty} \rightarrow \int_0^{\infty} d\omega_k, \quad (\text{C12a})$$

$$\begin{aligned} &\sum_{k=0}^{\infty} \int_0^t \frac{\gamma \Delta \omega}{\pi} c_+(s) e^{-i(\omega_k - \omega_+)(t-s)} ds \\ &\rightarrow \int_0^{\infty} \int_0^t 2\gamma c_+(s) e^{-i(\omega_k - \omega_+)(t-s)} ds \frac{d\omega_k}{2\pi} \\ &= \int_{-\omega_+}^{\infty} \int_0^t 2\gamma c_+(s) e^{-i\omega(t-s)} ds \frac{d\omega}{2\pi} \\ &\approx \int_{-\infty}^{\infty} \int_0^t 2\gamma c_+(s) e^{-i\omega(t-s)} ds \frac{d\omega}{2\pi} \\ &= \int_0^t 2\gamma c_+(s) \delta(t-s) ds = \frac{2\gamma c_+(t)}{2} = \gamma c_+(t). \end{aligned} \quad (\text{C12b})$$

Substituting (C11) and (C12) into (C10), we obtain

$$\dot{c}_+ = -\eta c_- d + \sqrt{2\gamma} a_+ - \gamma c_+, \quad (\text{C13})$$

$$\dot{c}_+ + \gamma c_+ + \eta c_- d = \sqrt{2\gamma} a_+. \quad (\text{C14})$$

By analogy we derive the equation for the input field a_- and present it in a similar form:

$$a_-(t) = \sum_{k=0}^{\infty} \sqrt{\frac{\Delta \omega}{2\pi}} b_k(0) e^{-i(\omega_k - \omega_-)t}. \quad (\text{C15})$$

It leads to the equation for the intracavity field c_- :

$$\dot{c}_- + \gamma c_- - \eta c_+ d^\dagger = \sqrt{2\gamma} a_-. \quad (\text{C16})$$

A similar equation can be derived for the amplitude $q(t)$ of the mechanical oscillator,

$$q(t) = \sum_{k=0}^{\infty} \sqrt{\frac{\Delta \omega}{2\pi}} b_{m,k}(0) e^{-i(\omega_k - \omega_+)t}, \quad (\text{C17})$$

and we get the following Langevine equation for the mechanical oscillator's quadrature d ,

$$\dot{d} + \gamma_m d - \eta^* c_+ c_-^\dagger = \sqrt{2\gamma_m} q. \quad (\text{C18})$$

To get the output relation we substitute (C9) into (C7a) and define the output fields as

$$b_+(t) = - \sum_{k=0}^{\infty} \sqrt{\frac{\Delta \omega}{2\pi}} b_k(\infty) e^{-i(\omega_k - \omega_+)t}, \quad (\text{C19})$$

$$b_-(t) = - \sum_{k=0}^{\infty} \sqrt{\frac{\Delta \omega}{2\pi}} b_k(\infty) e^{-i(\omega_k - \omega_+)t}. \quad (\text{C20})$$

This leads to

$$\dot{c}_+ - \gamma c_+ + \eta c_- d = \sqrt{2\gamma} b_+, \quad (\text{C21})$$

$$\dot{c}_- - \gamma c_- + \eta^* c_+ d^\dagger = \sqrt{2\gamma} b_-. \quad (\text{C22})$$

Utilizing pairs of equations, (C14) and (C21) as well as (C16) and (C22), we obtain the final expressions for the input-output relations:

$$b_+ = -a_+ + \sqrt{2\gamma} c_+, \quad (\text{C23})$$

$$b_- = -a_- + \sqrt{2\gamma} c_-. \quad (\text{C24})$$

Let us derive the commutation relations for the Fourier amplitudes of the operators. We introduce the Fourier transform of the field $a_+(t)$ using (C11):

$$a_+(\Omega) = \int_{-\infty}^{\infty} \sum_{k=0}^{\infty} \sqrt{\frac{\Delta \omega}{2\pi}} b_k(0) e^{-i(\omega_k - \omega_+ - \Omega)t} dt \quad (\text{C25a})$$

$$= \sum_{k=0}^{\infty} \sqrt{2\pi \Delta \omega} b_k(0) \delta(\Omega - \omega_k + \omega_+) \quad (\text{C25b})$$

This allows us to find the commutators (3.7):

$$\begin{aligned} &[a_+(\Omega), a_+^\dagger(\Omega')] \\ &= \sum_{k=0}^{\infty} 2\pi \Delta \omega [b_k(0), b_k^\dagger(0)] \\ &\quad \times \delta(\Omega - \omega_k + \omega_+) \delta(\Omega' - \omega_k + \omega_+) \\ &\rightarrow \int_{-\infty}^{\infty} 2\pi [b(0), b^\dagger(0)] \delta(\Omega - \omega) \delta(\Omega' - \omega) d\omega \\ &= 2\pi \delta(\Omega - \Omega'), \end{aligned} \quad (\text{C26a})$$

and it allows us to find the correlators (3.8):

$$\begin{aligned} &\langle a_+(\Omega), a_+^\dagger(\Omega') \rangle \\ &= \sum_{k=0}^{\infty} 2\pi \Delta \omega \langle b_k(0), b_k^\dagger(0) \rangle \delta \\ &\quad \times (\Omega - \omega_k + \omega_+) \delta(\Omega' - \omega_k + \omega_+) \\ &\rightarrow \int_{-\infty}^{\infty} 2\pi \langle b(0), b^\dagger(0) \rangle \delta(\Omega - \omega) \delta(\Omega' - \omega) d\omega \\ &= 2\pi \delta(\Omega - \Omega'). \end{aligned} \quad (\text{C27a})$$

Similar expressions can be derived for commutators and correlators of the optical a_- and mechanical q quantum amplitudes.

APPENDIX D: ACCOUNT OF PARASITIC SIDE BANDS

In this section we provide details of calculations taking into account the parasitic optical harmonics in the system. To do this, we use Hamiltonian equations generated by means of (2.4) and we replace $c_{\pm} \Rightarrow C_{\pm} + c_{\pm} + \tilde{c}_{\pm}$, where C_{\pm} represents mean-field amplitudes and $c_{\pm} + \tilde{c}_{\pm}$ represents the fluctuation parts. The term c_{\pm} was considered in the main part of the paper. The new term \tilde{c}_{\pm} has been introduced to reflect the generation of the parasitic sidebands.

The fluctuation fields in “+” and “-” cavities are not correlated with each other. Also, the sidebands described by c_{\pm} and \tilde{c}_{\pm} are not correlated because they are localized at different frequencies.

The terms proportional to \tilde{c}_{\pm} and corresponding to parasitic backaction can be written in a similar way if compared with the standard backaction terms. Fluctuations \tilde{c}_{\pm} are out of resonance; nevertheless, they are present in modes being impaired.

Using the rotating-wave approximation we derive the additional terms for the set of Hamilton equations (3.3c) for the mechanical operator

$$(\gamma_m - i\Omega)d(\Omega) = \eta[C_+c_-^\dagger(-\Omega) + C_-^*c_+(\Omega)] \quad (D1a)$$

$$- \eta[C_+^*\tilde{c}_-(\Omega) - C_- \tilde{c}_+^\dagger(-\Omega)] \quad (D1b)$$

$$+ \sqrt{2\gamma_m}q(\Omega) + if_s(\Omega), \quad (D1c)$$

where the terms in (D1b) describe the contributions due to the parasitic backaction. For example, the first term in (D1b) is derived as

$$C_+^*e^{i\omega_+t}\tilde{c}_-(\Omega)e^{-i(\omega_-+2\omega_m)t} = C_+^*\tilde{c}_-(\Omega)e^{-i\omega_m t} \quad (D2)$$

(see definition of $\tilde{c}_-(\Omega)$ in Fig. 3). Since the mechanical operator $d(\Omega)$ is multiplied by the same time-dependent rotation term $e^{-i\omega_m t}$ in the left-hand side of Eq. (D1), it can be removed.

The operators c_{\pm} obey (3.3). For the operators of the parasitic sidebands inside the cavity we derive

$$\begin{aligned} \tilde{c}_+(\Omega)(\gamma + i2\omega_m - i\Omega) &= \sqrt{2\gamma}\tilde{a}_+(\Omega) - \eta C_- d^\dagger(-\Omega), \\ \tilde{a}_+(\Omega) &= a_+(-2\omega_m + \Omega), \end{aligned} \quad (D3a)$$

$$\begin{aligned} \tilde{c}_-(\Omega)(\gamma - 2i\omega_m - i\Omega) &= \sqrt{2\gamma}\tilde{a}_-(\Omega) + \eta C_+ d(\Omega), \\ \tilde{a}_-(\Omega) &= a_-(2\omega_m + \Omega). \end{aligned} \quad (D3b)$$

For output amplitudes of parasitic sidebands we find

$$\tilde{b}_+(\Omega) = \frac{\gamma - 2i\omega_m + i\Omega}{\gamma + 2i\omega_m - i\Omega}\tilde{a}_+(\Omega) - \frac{\sqrt{2\gamma}\eta C_- d^\dagger(-\Omega)}{\gamma + 2i\omega_m - i\Omega}, \quad (D4a)$$

$$\tilde{b}_-(\Omega) = \frac{\gamma + 2i\omega_m + i\Omega}{\gamma - 2i\omega_m - i\Omega}\tilde{a}_-(\Omega) + \frac{\sqrt{2\gamma}\eta C_+ d(\Omega)}{\gamma - 2i\omega_m - i\Omega}. \quad (D4b)$$

Quadratures

Let us consider the case of the resonance probe light (3.12), find quadratures for parasitic optical harmonics, and rewrite the expression (D1) for the mechanical quadratures as

$$\begin{aligned} \tilde{c}_{a\pm} &= \frac{\tilde{c}_{\pm}(\Omega) + \tilde{c}_{\pm}^\dagger(-\Omega)}{\sqrt{2}}, \quad \tilde{c}_{\phi\pm} \\ &= \frac{\tilde{c}_{\pm}(\Omega) - \tilde{c}_{\pm}^\dagger(-\Omega)}{i\sqrt{2}}, \end{aligned} \quad (D5a)$$

$$\begin{aligned} (\gamma_m - i\Omega)d_a &= \eta C[c_{a-} + c_{a+}] - \eta C[\tilde{c}_{a-} - \tilde{c}_{a+}] \\ &\quad + \sqrt{2\gamma_m}q_a - f_{\phi s}, \end{aligned} \quad (D5b)$$

$$\begin{aligned} (\gamma_m - i\Omega)d_\phi &= \eta C[-c_{\phi-} + c_{\phi+}] - \eta C[\tilde{c}_{\phi-} + \tilde{c}_{\phi+}] \\ &\quad + \sqrt{2\gamma_m}q_\phi + f_{as}. \end{aligned} \quad (D5c)$$

Substituting (D5) into (3.3a) and (3.3b), we get

$$\begin{aligned} c_{+a} &= \frac{\sqrt{2\gamma}a_{a+}}{\gamma - i\Omega} - \frac{\eta^2 C^2[c_{a-} + c_{a+} - \tilde{c}_{a-} - \tilde{c}_{a+}]}{(\gamma_m - i\Omega)(\gamma - i\Omega)} \\ &\quad - \eta C \frac{\sqrt{2\gamma_m}q_a - f_{\phi s}}{(\gamma_m - i\Omega)(\gamma - i\Omega)}, \end{aligned} \quad (D6a)$$

$$\begin{aligned} c_{-a} &= \frac{\sqrt{2\gamma}a_{a-}}{\gamma - i\Omega} + \frac{\eta^2 C^2[c_{a-} + c_{a+} - \tilde{c}_{a-} - \tilde{c}_{a+}]}{(\gamma_m - i\Omega)(\gamma - i\Omega)} \\ &\quad + \eta C \frac{\sqrt{2\gamma_m}q_a - f_{\phi s}}{(\gamma_m - i\Omega)(\gamma - i\Omega)}, \end{aligned} \quad (D6b)$$

$$\begin{aligned} c_{+\phi} &= \frac{\sqrt{2\gamma}a_{\phi+}}{\gamma - i\Omega} - \frac{\eta^2 C^2[-c_{\phi-} + c_{\phi+} - \tilde{c}_{\phi-} + \tilde{c}_{\phi+}]}{(\gamma_m - i\Omega)(\gamma - i\Omega)} \\ &\quad - \eta C \frac{\sqrt{2\gamma_m}q_\phi + f_{as}}{(\gamma_m - i\Omega)(\gamma - i\Omega)}, \end{aligned} \quad (D6c)$$

$$\begin{aligned} c_{-\phi} &= \frac{\sqrt{2\gamma}a_{\phi-}}{\gamma - i\Omega} - \frac{\eta^2 C^2[-c_{\phi-} + c_{\phi+} - \tilde{c}_{\phi-} + \tilde{c}_{\phi+}]}{(\gamma_m - i\Omega)(\gamma - i\Omega)} \\ &\quad - \eta C \frac{\sqrt{2\gamma_m}q_\phi + f_{as}}{(\gamma_m - i\Omega)(\gamma - i\Omega)}. \end{aligned} \quad (D6d)$$

We introduce sum and difference quadratures for the parasitic sidebands, similarly to (3.15), (3.16), and (3.17):

$$\tilde{g}_{a\pm} = \frac{\tilde{c}_{+a} \pm \tilde{c}_{-a}}{\sqrt{2}}, \quad \tilde{g}_{\phi\pm} = \frac{\tilde{c}_{+\phi} \pm \tilde{c}_{-\phi}}{\sqrt{2}}, \quad (D7a)$$

$$\tilde{\alpha}_{a\pm} = \frac{\tilde{a}_{+a} \pm \tilde{a}_{-a}}{\sqrt{2}}, \quad \tilde{\alpha}_{\phi\pm} = \frac{\tilde{a}_{+\phi} \pm \tilde{a}_{-\phi}}{\sqrt{2}}, \quad (D7b)$$

$$\tilde{\beta}_{a\pm} = \frac{\tilde{b}_{+a} \pm \tilde{b}_{-a}}{\sqrt{2}}, \quad \tilde{\beta}_{\phi\pm} = \frac{\tilde{b}_{+\phi} \pm \tilde{b}_{-\phi}}{\sqrt{2}}, \quad (D7c)$$

and we arrive at the following expressions for the sum and difference quadratures:

$$g_{a+} = \frac{\sqrt{2\gamma}\alpha_{a+}}{\gamma - i\Omega}, \quad (D8a)$$

$$\begin{aligned} g_{a-} &= \frac{\sqrt{2\gamma}\alpha_{a-}}{\gamma - i\Omega} - \frac{2\eta^2 C^2[g_{a+} - \tilde{g}_{a+}]}{(\gamma_m - i\Omega)(\gamma - i\Omega)} \\ &\quad - \sqrt{2}\eta C \frac{\sqrt{2\gamma_m}q_a - f_{\phi s}}{(\gamma_m - i\Omega)(\gamma - i\Omega)}, \end{aligned} \quad (D8b)$$

$$g_{\phi-} = \frac{\sqrt{2\gamma} \alpha_{\phi-}}{\gamma - i\Omega}, \quad (\text{D8c})$$

$$g_{\phi+} = \frac{\sqrt{2\gamma} \alpha_{\phi+}}{\gamma - i\Omega} - \frac{2\eta^2 C^2 [g_{\phi-} + \tilde{g}_{\phi-}]}{(\gamma_m - i\Omega)(\gamma - i\Omega)} - \sqrt{2} \eta C \frac{\sqrt{2\gamma_m} q_\phi + f_{as}}{(\gamma_m - i\Omega)(\gamma - i\Omega)}. \quad (\text{D8d})$$

At the next step we evaluate the sum and difference quadratures of sidebands using (D3):

$$\tilde{g}_{a+} = \frac{\sqrt{2\gamma}}{2} \left(\frac{\tilde{a}_+(\Omega) + \tilde{a}_+^\dagger(-\Omega)}{(\gamma + 2i\omega_m - i\Omega)} + \frac{\tilde{a}_+^\dagger(-\Omega) + \tilde{a}_-(\Omega)}{(\gamma - 2i\omega_m - i\Omega)} \right), \quad (\text{D9a})$$

$$\tilde{g}_{\phi-} = \frac{\sqrt{2\gamma}}{i2} \left(\frac{\tilde{a}_+(\Omega) + \tilde{a}_+^\dagger(-\Omega)}{(\gamma + 2i\omega_m - i\Omega)} - \frac{\tilde{a}_+^\dagger(-\Omega) + \tilde{a}_-(\Omega)}{(\gamma - 2i\omega_m - i\Omega)} \right). \quad (\text{D9b})$$

The combinations above do not contain any information on the displacement of the mechanical oscillator.

For output sum and difference quadratures, taking advantage of Eq. (3.3d), we obtain

$$\beta_{a-} = \frac{\gamma + i\Omega}{\gamma - i\Omega} \alpha_{a-} - \sqrt{2\gamma} \frac{2\eta^2 C^2 [g_{a+} - \tilde{g}_{a+}]}{(\gamma_m - i\Omega)(\gamma - i\Omega)} - 2\sqrt{\gamma} \eta C \frac{\sqrt{2\gamma_m} q_a - f_{\phi s}}{(\gamma_m - i\Omega)(\gamma - i\Omega)}, \quad (\text{D10a})$$

$$\beta_{a+} = \frac{\gamma + i\Omega}{\gamma - i\Omega} \alpha_{a+}, \quad (\text{D10b})$$

$$\beta_{\phi+} = \frac{\gamma + i\Omega}{\gamma - i\Omega} \alpha_{\phi+} - \sqrt{2\gamma} \frac{2\eta^2 C^2 [g_{\phi-} + \tilde{g}_{\phi-}]}{(\gamma_m - i\Omega)(\gamma - i\Omega)} - 2\sqrt{\gamma} \eta C \frac{\sqrt{2\gamma_m} q_\phi + f_{as}}{(\gamma_m - i\Omega)(\gamma - i\Omega)}, \quad (\text{D10c})$$

$$g_{\phi-} = \frac{\gamma + i\Omega}{\gamma - i\Omega} \alpha_{\phi-}. \quad (\text{D10d})$$

Finally, we rewrite β_{a+} after compensation of the main backaction term as (4.1).

We see that one can subtract completely the main (proportional to α_{a+}) term of the backaction. The contribution of the parasitic harmonic (proportional to \tilde{g}_{a+}) into the backaction limits the sensitivity of the measurement in this case. In the following section we discuss a possibility of the reduction of their impact.

APPENDIX E: REDUCTION OF THE RESIDUAL BACKACTION

Using (D9) we find

$$\tilde{\beta}_{a+} = \frac{1}{2} \left\{ \frac{\gamma - 2i\omega_m + i\Omega}{\gamma + 2i\omega_m - i\Omega} [\tilde{a}_+(\Omega) + \tilde{a}_+^\dagger(-\Omega)] + \frac{\gamma + 2i\omega_m + i\Omega}{\gamma - 2i\omega_m - i\Omega} [\tilde{a}_+^\dagger(-\Omega) + \tilde{a}_-(\Omega)] \right\}, \quad (\text{E1a})$$

$$\tilde{\beta}_{\phi-} = \frac{1}{2i} \left\{ \frac{\gamma - 2i\omega_m + i\Omega}{\gamma + 2i\omega_m - i\Omega} [\tilde{a}_+(\Omega) + \tilde{a}_+^\dagger(-\Omega)] - \frac{\gamma + 2i\omega_m - i\Omega}{\gamma - 2i\omega_m + i\Omega} [\tilde{a}_+^\dagger(-\Omega) + \tilde{a}_-(\Omega)] \right\}. \quad (\text{E1b})$$

In order to compensate for the ‘‘tilde’’ terms we have to measure a combination of arbitrary quadratures defined by phases φ_\pm :

$$\tilde{b}_{+\varphi} = \frac{\tilde{b}_+(\Omega)e^{i\varphi_+} + \tilde{b}_+^\dagger(\Omega)e^{-i\varphi_+}}{\sqrt{2}}, \quad (\text{E2a})$$

$$\tilde{b}_{-\varphi} = \frac{\tilde{b}_-(\Omega)e^{i\varphi_-} + \tilde{b}_-^\dagger(\Omega)e^{-i\varphi_-}}{\sqrt{2}}. \quad (\text{E2b})$$

In order to remove parasitic terms we have to define the phases as follows:

$$\begin{aligned} \varphi_+ = -\varphi_- = \varphi &\Rightarrow \frac{\tilde{b}_{+\varphi} + \tilde{b}_{-\varphi}}{\sqrt{2}} \\ &= \frac{\gamma - i2\omega_m + i\Omega}{2(\gamma + i2\omega_m - i\Omega)} (\tilde{a}_+(\Omega) + \tilde{a}_+^\dagger(-\Omega)) e^{i\varphi} \\ &\quad + \frac{\gamma + i2\omega_m + i\Omega}{2(\gamma - i2\omega_m - i\Omega)} (\tilde{a}_-(\Omega) + \tilde{a}_+^\dagger(-\Omega)) e^{-i\varphi}. \end{aligned} \quad (\text{E2c})$$

We get for φ an approximate expression:

$$(\gamma - i2\omega_m + i\Omega)e^{i\varphi} \simeq \text{const} \Rightarrow e^{i\varphi} = \sqrt{\frac{\gamma + 2i\omega_m}{\gamma - 2i\omega_m}}. \quad (\text{E2d})$$

Performing the same procedure we developed for the main harmonics of the probe light, we find that the impact of the parasitic harmonics can be reduced by $R \simeq \Omega/2\omega_m$ [assuming the validity of conditions (2.2)]. After the compensation we obtain

$$\begin{aligned} \beta_{a-} = \frac{\xi\sqrt{\mathcal{K}}}{(\gamma_m - i\Omega)} &\left\{ \frac{(\gamma_m - i\Omega)}{\sqrt{\mathcal{K}}} \alpha_{a-} - \sqrt{\mathcal{K}} \alpha_{a+} \right. \\ &\left. + \sqrt{\mathcal{K}} \frac{(\gamma - i\Omega)}{\sqrt{2\gamma}} \tilde{g}_{a+} R - \sqrt{\xi^{-1}} [\sqrt{2\gamma_m} q_a - f_{\phi s}] \right\}. \end{aligned} \quad (\text{E3})$$

instead of (4.1). The first term in braces, α_{a-} , results from the quantum measurement noise and the second term, α_{a+} , describes backaction that can be removed from the measurement results. The backaction term due to the parasitic harmonics can be reduced. Optimization of contributions of these terms defines the ultimate sensitivity of the measurement technique that is better than that of the SQL.

- [1] B. P. Abbott *et al.* (KAGRA Collaboration, LIGO Scientific Collaboration and Virgo Collaboration), Prospects for observing and localizing gravitational-wave transients with Advanced LIGO, Advanced Virgo and KAGRA, *Living Rev. Relativ.* **23**, 3 (2020).
- [2] J. Aasi *et al.* (LIGO Scientific Collaboration), Characterization of the LIGO detectors during their sixth science run, *Classical Quantum Gravity* **32**, 115012 (2015).
- [3] D. Martynov *et al.*, Sensitivity of the Advanced LIGO detectors at the beginning of gravitational wave astronomy, *Phys. Rev. D* **93**, 112004 (2016).
- [4] F. Asernese *et al.*, Advanced Virgo: A 2nd generation interferometric gravitational wave detector, *Classical Quantum Gravity* **32**, 024001 (2015).
- [5] K. L. Dooley, J. R. Leong, T. Adams, C. Affeldt, A. Bisht, C. Bogan, J. Degallaix, C. Graf, S. Hild, and J. Hough, GEO 600 and the GEO-HF upgrade program: successes and challenges, *Classical Quantum Gravity* **33**, 075009 (2016).
- [6] Y. Aso, Y. Michimura, K. Somiya, M. Ando, O. Miyakawa, T. Sekiguchi, D. Tatsumi, and H. Yamamoto, Interferometer design of the KAGRA gravitational wave detector, *Phys. Rev. D* **88**, 043007 (2013).
- [7] S. Forstner, S. Prams, J. Knittel, E. D. van Ooijen, J. D. Swaim, G. I. Harris, A. Szorkovszky, W. P. Bowen, and H. Rubinsztein-Dunlop, Cavity Optomechanical Magnetometer, *Phys. Rev. Lett.* **108**, 120801 (2012).
- [8] B.-B. Li, J. Břlek, U. Hoff, L. Madsen, S. Forstner, V. Prakash, C. Schafermeier, T. Gehring, W. Bowen, and U. Andersen, Quantum enhanced optomechanical magnetometry, *Optica* **5**, 850 (2018).
- [9] M. Wu, A. C. Hryciw, C. Healey, D. P. Lake, H. Jayakumar, M. R. Freeman, J. P. Davis, and P. E. Barclay, Dissipative and Dispersive Optomechanics in a Nanocavity Torque Sensor, *Phys. Rev. X* **4**, 021052 (2014).
- [10] P. H. Kim, B. D. Hauer, C. Doolin, F. Souris, and J. P. Davis, Approaching the standard quantum limit of mechanical torque sensing, *Nat. Commun.* **7**, 13165 (2016).
- [11] J. Ahn, Z. Xu, J. Bang, P. Ju, X. Gao, and T. Li, Ultrasensitive torque detection with an optically levitated nanorotor, *Nat. Nanotechnol.* **15**, 89 (2020).
- [12] V. B. Braginsky, Classic and quantum limits for detection of weak force on acting on macroscopic oscillator, *Sov. Phys. JETP* **26**, 831 (1968).
- [13] V. B. Braginsky and F. Ya. Khalili, *Quantum Measurement* (Cambridge University, Cambridge, England, 1992).
- [14] V. B. Braginsky and F. Ya. Khalili, Gravitational wave antenna with QND speed meter, *Phys. Lett. A* **147**, 251 (1990).
- [15] V. B. Braginsky, M. L. Gorodetsky, F. Y. Khalili, and K. S. Thorne, Dual-resonator speed meter for a free test mass, *Phys. Rev. D* **61**, 044002 (2000).
- [16] V. B. Braginsky and F. Ya. Khalili, Low noise rigidity in quantum measurements, *Phys. Lett. A* **257**, 241 (1999).
- [17] F. Ya. Khalili, Frequency-dependent rigidity in large-scale interferometric gravitational-wave detectors, *Phys. Lett. A* **288**, 251 (2001).
- [18] J. Cripe, T. Cullen, Y. Chen, P. Heu, D. Follman, G. D. Cole, and T. Corbitt, Quantum Backaction Cancellation in the Audio Band, *Phys. Rev. X* **10**, 031065 (2020).
- [19] The LIGO Scientific Collaboration, A gravitational wave observatory operating beyond the quantum shot-noise limit, *Nat. Phys.* **7**, 962 (2011).
- [20] LIGO Scientific Collaboration and Virgo Collaboration, Enhanced sensitivity of the LIGO gravitational wave detector by using squeezed states of light, *Nat. Photonics* **7**, 613 (2013).
- [21] V. Tse *et al.*, Quantum-Enhanced Advanced LIGO Detectors in the Era of Gravitational-Wave Astronomy, *Phys. Rev. Lett.* **123**, 231107 (2019).
- [22] F. Asernese *et al.* (Virgo Collaboration), Increasing the Astrophysical Reach of the Advanced Virgo Detector via the Application of Squeezed Vacuum States of Light, *Phys. Rev. Lett.* **123**, 231108 (2019).
- [23] M. Yap, J. Cripe, G. Mansell *et al.*, Broadband reduction of quantum radiation pressure noise via squeezed light injection, *Nat. Photonics* **14**, 19 (2020).
- [24] H. Yu, L. McCuller, M. Tse *et al.*, Quantum correlations between light and the kilogram-mass mirrors of LIGO, *Nature (London)* **583**, 43 (2020).
- [25] J. Cripe, N. Aggarwal, R. Lanza *et al.*, Measurement of quantum back action in the audio band at room temperature, *Nature (London)* **568**, 364 (2019).
- [26] S. P. Vyatchanin and A. B. Matsko, Quantum limit of force measurement, *Sov. Phys JETP* **77**, 218 (1993).
- [27] S. Vyatchanin and E. Zubova, Quantum variation measurement of force, *Phys. Lett. A* **201**, 269 (1995).
- [28] H. J. Kimble, Y. Levin, A. B. Matsko, K. S. Thorne, and S. P. Vyatchanin, Conversion of conventional gravitational-wave interferometers into QND interferometers by modifying input and/or output optics, *Phys. Rev. D* **65**, 022002 (2001).
- [29] M. Tsang and C. M. Caves, Coherent Quantum-Noise Cancellation for Optomechanical Sensors, *Phys. Rev. Lett.* **105**, 123601 (2010).
- [30] E. Polzik and K. Hammerer, Trajectories without quantum uncertainties, *Ann. Phys.* **527**, A15 (2014).
- [31] C. Moller, R. Thomas, G. Vasilakis, E. Zeuthen, Y. Tsaturyan, M. Balabas, K. Jensen, A. Schliesser, K. Hammerer, and E. Polzik, Quantum back-action-evading measurement of motion in a negative mass reference frame, *Nature (London)* **547**, 191 (2017).
- [32] A. B. Matsko, V. V. Kozlov, and M. O. Scully, Backaction Cancellation in Quantum Nondemolition Measurement of Optical Solitons, *Phys. Rev. Lett.* **82**, 3244 (1999).
- [33] V. Braginsky, Y. Vorontsov, and K. Thorne, Quantum nondemolition measurements, *Science* **209**, 547 (1980).
- [34] V. B. Braginskii, Yu. I. Vorontsov, and F. Y. Khalili, Optimal quantum measurements in detectors of gravitation radiation, *JETP Lett.* **27**, 276 (1978).
- [35] A. Clerk, F. Marquardt, and K. Jacobs, Back-action evasion and squeezing of a mechanical resonator using a cavity detector, *New J. Phys.* **10**, 095010 (2008).
- [36] E. Wollman, C. Lei, A. Weinstein, J. Suh, A. Kronwald, F. Marquardt, A. Clerk, and K. Schwab, Quantum squeezing of motion in a mechanical resonator, *Science* **349**, 952 (2015).
- [37] J.-M. Pirkkalainen, E. Damskagg, M. Brandt, F. Massel, and M. A. Sillanpaa, Squeezing of Quantum Noise of Motion in a Micromechanical Resonator, *Phys. Rev. Lett.* **115**, 243601 (2015).

- [38] L. F. Buchmann, S. Schreppler, J. Kohler, N. Spethmann, and D. M. Stamper-Kurn, Complex Squeezing and Force Measurement Beyond the Standard Quantum Limit, *Phys. Rev. Lett.* **117**, 030801 (2016).
- [39] S. Vyatchanin and A. Matsko, On sensitivity limitations of a dichromatic optical detection of a classical mechanical force, *J. Opt. Soc. Am. B* **35**, 1970 (2018).
- [40] M. H. Wimmer, D. Steinmeyer, K. Hammerer, and M. Heurs, Coherent cancellation of backaction noise in optomechanical force measurements, *Phys. Rev. A* **89**, 053836 (2014).
- [41] M. L. Povinelli, M. Loncar, M. Ibanescu, E. J. Smythe, S. G. Johnson, F. Capasso, and J. D. Joannopoulos, Evanescent-wave bonding between optical waveguides, *Opt. Lett.* **30**, 3042 (2005).
- [42] A. V. Maslov, V. N. Astratov, and M. I. Bakunov, Resonant propulsion of a microparticle by a surface wave, *Phys. Rev. A* **87**, 053848 (2013).
- [43] S. P. Vyatchanin and A. B. Matsko, Quantum variation scheme of measurement of force and compensation of backaction, *Sov. Phys. JETP* **82**, 107 (1996).
- [44] A. B. Matsko and S. P. Vyatchanin, A ponderomotive scheme for QND measurement of quadrature component, *Appl. Phys. B* **64**, 167 (1997).
- [45] X. Li, M. Korobko, Y. Ma, R. Schnabel, and Y. Chen, Coherent coupling completing an unambiguous optomechanical classification framework, *Phys. Rev. A* **100**, 053855 (2019).
- [46] A. Beccari, D. A. Visani, S. A. Fedorov, M. J. Beryhi, V. Boureau, N. J. Engelsen, and T. J. Kippenberg, Strained crystalline nanomechanical resonators with ultralow dissipation, [arXiv:2107.02124](https://arxiv.org/abs/2107.02124).
- [47] S. A. Fedorov, N. J. Engelsen, A. H. Ghadimi, M. J. Beryhi, R. Schilling, D. J. Wilson, and T. J. Kippenberg, Generalized dissipation dilution in strained mechanical resonators, *Phys. Rev. B* **99**, 054107 (2019).
- [48] D. Walls and G. Milburn, *Quantum Optics* (Springer-Verlag, Berlin, 2008).